Eur. Phys. J. A **26**, 277–284 (2005)
DOI 10.1140/epja/i2004-10307-2

THE EUROPEAN PHYSICAL JOURNAL A

The centrality dependence of transverse-energy and charged-particle multiplicity at RHIC: Statistical model analysis

D. Prorok[a]

Institute of Theoretical Physics, University of Wrocław, Pl. Maksa Borna 9, 50-204 Wrocław, Poland

Received: 28 December 2004 / Revised version: 5 September 2005 /
Published online: 22 November 2005 –
Communicated by A. Molinari

Abstract. The transverse-energy and charged-particle multiplicity at midrapidity and their ratio are evaluated in a statistical model with the longitudinal and transverse flows for different centrality bins at RHIC at $\sqrt{s_{NN}} = 130$ and 200 GeV. Full description of decays of hadron resonances is applied in these estimations. The predictions of the model at the freeze-out parameters, which were determined from measured particle yields and p_T spectra, agree qualitatively well with the experimental data. The observed overestimation of the ratio can be explained for more central collisions by the redefinition of $\mathrm{d}N_{\mathrm{ch}}/\mathrm{d}\eta|_{\mathrm{mid}}$.

PACS. 25.75.-q Relativistic heavy-ion collisions – 25.75.Dw Particle and resonance production – 24.10.Pa Thermal and statistical models – 24.10.Jv Relativistic models

1 Introduction

In the previous paper [1] the extensive analysis of two measured global variables, transverse-energy ($\mathrm{d}E_T/\mathrm{d}\eta|_{\mathrm{mid}}$) and charged-particle multiplicity ($\mathrm{d}N_{\mathrm{ch}}/\mathrm{d}\eta|_{\mathrm{mid}}$) densities at midrapidity, was delivered. The analysis was done in the framework of the single freeze-out statistical model [2–4] for the most central-collision cases of AGS, SPS and RHIC. Now the same method will be applied in the examination of the centrality dependence of the above-mentioned variables and their ratio. The main idea of this method is as follows. Thermal and geometric parameters of the model are determined from fits to the particle yield ratios and p_T spectra, respectively. Then, with the use of these parameters both densities, $\mathrm{d}E_T/\mathrm{d}\eta$ and $\mathrm{d}N_{\mathrm{ch}}/\mathrm{d}\eta$, can be estimated numerically and compared with the data. The first part of this two-step prescription has been already done for the existing midrapidity data for different centrality bins at RHIC at $\sqrt{s_{NN}} = 130$ and 200 GeV [5,6]. In the present paper the second step will be performed, namely the estimations of $\mathrm{d}E_T/\mathrm{d}\eta|_{\mathrm{mid}}$ and $\mathrm{d}N_{\mathrm{ch}}/\mathrm{d}\eta|_{\mathrm{mid}}$ for these centralities and comparison with the data reported in refs. [7–10]. The main reason for doing it is that the transverse-energy and charged-particle multiplicity measurements are independent of hadron spectroscopy (in particular, no particle identification is necessary); therefore they could be used as an additional test of the self-consistency of a statistical model. There is also an additional pragmatic reason: predictions of the variety of theoretical models were confronted with the data in [10], but none of these models was a statistical model.

The experimentally measured transverse energy is defined as

$$E_T = \sum_{i=1}^{L} \hat{E}_i \cdot \sin\theta_i \ , \tag{1}$$

where θ_i is the polar angle, $\hat{E}_i$ denotes $E_i - m_N$ (m_N means the nucleon mass) for baryons, $E_i + m_N$ for antibaryons and the total energy E_i for all other particles, and the sum is taken over all L emitted particles [10].

As a statistical model the single freeze-out model is applied (for details see [5]). The model succeeded in the accurate description of ratios and p_T spectra of particles measured at RHIC [2–4]. The main postulate of the model is the simultaneous occurrence of chemical and thermal freeze-outs, which means that the possible elastic interactions after the chemical freeze-out are neglected. The conditions for the freeze-out are expressed by values of two independent thermal parameters: T and μ_B. The strangeness chemical potential μ_S is determined from the requirement that the overall strangeness equals zero.

The second basic feature of the model is the complete treatment of resonance decays. This means that the final distribution of a given particle consists not only of the thermal part but also of contributions from all possible decays and cascades.

[a] e-mail: prorok@ift.uni.wroc.pl

2 Foundations of the single freeze-out model

The main assumptions of the model are the following. A noninteracting gas of stable hadrons and resonances at chemical and thermal equilibrium appears at the latter stages of a heavy-ion collision. The gas cools and expands, and after reaching the freeze-out point it ceases. The chemical and thermal freeze-outs take place simultaneously. All confirmed resonances up to a mass of 2 GeV from the Particle Data Tables [11], together with stable hadrons, are constituents of the gas. The freeze-out hypersurface is defined by the equation

$$\tau = \sqrt{t^2 - r_x^2 - r_y^2 - r_z^2} = \text{const} \, . \tag{2}$$

The four-velocity of an element of the freeze-out hypersurface is proportional to its coordinate

$$u^\mu = \frac{x^\mu}{\tau} = \frac{t}{\tau} \, \left(1, \frac{r_x}{t}, \frac{r_y}{t}, \frac{r_z}{t}\right) \, . \tag{3}$$

The following parameterization of the hypersurface is chosen:

$$\begin{aligned} t &= \tau \cosh\alpha_\parallel \cosh\alpha_\perp \, , \quad & r_x &= \tau \sinh\alpha_\perp \cos\phi \, , \\ r_y &= \tau \sinh\alpha_\perp \sin\phi \, , & r_z &= \tau \sinh\alpha_\parallel \cosh\alpha_\perp \, , \end{aligned} \tag{4}$$

where $\alpha_\parallel$ is the rapidity of the element, $\alpha_\parallel = \tanh^{-1}(r_z/t)$, and $\alpha_\perp$ controls the transverse radius:

$$r = \sqrt{r_x^2 + r_y^2} = \tau \sinh\alpha_\perp . \tag{5}$$

The transverse size is restricted by the condition $r < \rho_{\max}$. This means that two new parameters of the model have been introduced, *i.e.* τ and $\rho_{\max}$, which are connected with the geometry of the freeze-out hypersurface.

The invariant distribution of the measured particles of species i has the form [3,4]

$$\frac{\mathrm{d}N_i}{\mathrm{d}^2p_T \, \mathrm{d}y} = \int p^\mu \mathrm{d}\sigma_\mu \, f_i(p\cdot u) \, , \tag{6}$$

where $\mathrm{d}\sigma_\mu$ is the normal vector on a freeze-out hypersurface, $p\cdot u = p^\mu u_\mu$, u_μ is the four-velocity of a fluid element and f_i is the final momentum distribution of the particle in question. The final distribution means here that f_i is the sum of primordial and simple and sequential decay contributions to the particle distribution. The primordial part of f_i is given by a Bose-Einstein or a Fermi-Dirac distribution at the freeze-out. A decay contribution is a one-dimensional or multidimensional integral of the momentum distribution of a decaying resonance (the exact formulae are obtained from the elementary kinematics of a many-body decay or the superposition of such decays, for details see [5] and the appendix in [1]). The resonance is a constituent of the hadron gas and its distribution is also given by the Bose-Einstein (Fermi-Dirac) distribution function. Therefore, the final distribution f_i depends explicitly on T and μ_B.

With the use of eqs. (3) and (4), the invariant distribution (6) takes the following form:

$$\begin{aligned} \frac{\mathrm{d}N_i}{\mathrm{d}^2p_T \, \mathrm{d}y} = \tau^3 \int\limits_{-\infty}^{+\infty} \mathrm{d}\alpha_\parallel \int\limits_0^{\rho_{\max}/\tau} \sinh\alpha_\perp \mathrm{d}(\sinh\alpha_\perp) \\ \times \int\limits_0^{2\pi} \mathrm{d}\xi \; p\cdot u \; f_i(p\cdot u) \, , \end{aligned} \tag{7}$$

where

$$p\cdot u = m_T \cosh\alpha_\parallel \cosh\alpha_\perp - p_T \cos\xi \sinh\alpha_\perp \, . \tag{8}$$

Note that the above distribution is explicitly boost invariant.

The pseudo-rapidity density of particle species i is given by

$$\frac{\mathrm{d}N_i}{\mathrm{d}\eta} = \int \mathrm{d}^2p_T \, \frac{\mathrm{d}y}{\mathrm{d}\eta} \, \frac{\mathrm{d}N_i}{\mathrm{d}^2p_T \, \mathrm{d}y} = \int \mathrm{d}^2p_T \, \frac{p}{E_i} \, \frac{\mathrm{d}N_i}{\mathrm{d}^2p_T \, \mathrm{d}y} \, . \tag{9}$$

Analogously, the transverse-energy pseudo-rapidity density for the same species can be written as

$$\begin{aligned} \frac{\mathrm{d}E_{T,i}}{\mathrm{d}\eta} = \int \mathrm{d}^2p_T \; \hat{E}_i \cdot \frac{p_T}{p} \, \frac{\mathrm{d}y}{\mathrm{d}\eta} \, \frac{\mathrm{d}N_i}{\mathrm{d}^2p_T \, \mathrm{d}y} = \\ \int \mathrm{d}^2p_T \; p_T \, \frac{\hat{E}_i}{E_i} \, \frac{\mathrm{d}N_i}{\mathrm{d}^2p_T \, \mathrm{d}y} \, . \end{aligned} \tag{10}$$

For the quantities at midrapidity one has (in the c.m.s., which is the RHIC frame of reference)

$$\frac{\mathrm{d}N_i}{\mathrm{d}\eta} \Big|_{\mathrm{mid}} = \int \mathrm{d}^2p_T \, \frac{p_T}{m_T} \, \frac{\mathrm{d}N_i}{\mathrm{d}^2p_T \, \mathrm{d}y} \, , \tag{11}$$

$$\frac{\mathrm{d}E_{T,i}}{\mathrm{d}\eta} \Big|_{\mathrm{mid}} = \begin{cases} \int \mathrm{d}^2p_T \; p_T \; \frac{m_T - m_N}{m_T} \; \frac{\mathrm{d}N_i}{\mathrm{d}^2p_T \, \mathrm{d}y} \, , & i = \text{baryon} \, , \\ \int \mathrm{d}^2p_T \; p_T \; \frac{m_T + m_N}{m_T} \; \frac{\mathrm{d}N_i}{\mathrm{d}^2p_T \, \mathrm{d}y} \, , & i = \text{antibaryon} \, , \\ \int \mathrm{d}^2p_T \; p_T \; \frac{\mathrm{d}N_i}{\mathrm{d}^2p_T \, \mathrm{d}y} \, , & i = \text{others} \, . \end{cases} \tag{12}$$

Note that for the older data from RHIC at $\sqrt{s_{NN}} = 130$ GeV [8] the *antibaryon* case is not distinguished and the corresponding expression for the transverse-energy density is the same as for all other particles.

The overall charged-particle and transverse-energy densities can be expressed as

$$\frac{\mathrm{d}N_{\mathrm{ch}}}{\mathrm{d}\eta} \Big|_{\mathrm{mid}} = \sum_{i\in B} \frac{\mathrm{d}N_i}{\mathrm{d}\eta} \Big|_{\mathrm{mid}} \, , \tag{13}$$

$$\frac{\mathrm{d}E_T}{\mathrm{d}\eta} \Big|_{\mathrm{mid}} = \sum_{i\in A} \frac{\mathrm{d}E_{T,i}}{\mathrm{d}\eta} \Big|_{\mathrm{mid}} \, , \tag{14}$$

where A and B ($B \subset A$) denote sets of species of finally detected particles, namely the set of charged particles B comprises π^+, π^-, K^+, K^-, p and $\bar{p}$, whereas A also includes photons, K^0_L, n and $\bar{n}$ [8].

3 Summary of the fit procedure

Analyses of the particle ratios and p_T spectra at various centralities in the framework of the single freeze-out model were done for RHIC in [5,6]. Here is the brief summary of this approach. It proceeds in two steps. First, thermal parameters T and μ_B are fitted with the use of the experimental ratios of hadron multiplicities at midrapidity. After then two next parameters, τ and $\rho_{\max}$, are determined from the simultaneous fit to the transverse-momentum spectra of $\pi^{\pm}$, $K^{\pm}$, p and $\bar{p}$. The fits are performed with the help of the χ^2 method. For the k-th measured quantity $R_k^{\exp}$ and its theoretical equivalent $R_k^{\rm th}(\alpha_1,\ldots,\alpha_l)$, which depends on l parameters $\alpha_1,\ldots,\alpha_l$, the χ^2-function is defined as

$$\chi^2(\alpha_1,\ldots,\alpha_l)=\sum_{k=1}^{n}\frac{(R_k^{\exp}-R_k^{\rm th}(\alpha_1,\ldots,\alpha_l))^2}{\sigma_k^2}\ , \quad (15)$$

where σ_k is the error of the k-th measurement and n is the total number of data points. The fitted values of the parameters mean the values at which χ^2 has a minimum.

To determine T and μ_B the k-th measured ratio of hadron multiplicities at midrapidity is put into eq. (15) as the measured quantity:

$$R_k^{\exp}=\frac{{\rm d}N_i^{\exp}/{\rm d}y}{{\rm d}N_j^{\exp}/{\rm d}y}\Big|_{\rm mid}\ . \quad (16)$$

In the case of a boost-invariant model (as here), the theoretical equivalent $R_k^{\rm th}(T,\mu_B)$ is given by

$$R_k^{\rm th}(T,\mu_B)=\frac{{\rm d}N_i^{\rm th}/{\rm d}y}{{\rm d}N_j^{\rm th}/{\rm d}y}\Big|_{\rm mid}=\frac{N_i^{\rm th}}{N_j^{\rm th}}=\frac{n_i(T,\mu_B)}{n_j(T,\mu_B)}\ , \quad (17)$$

where $n_i(T,\mu_B)$ is the final density of particle species i calculated for a static gas. The last equality follows from the assumption that the temperature and chemical potentials are constant on the freeze-out hypersurface. Then the volume of the hypersurface factorizes when the invariant distribution (6) is integrated formally over all momenta to obtain the total multiplicity $N_i^{\rm th}$ (for details see [5]). The final density means here that it collects all decay contributions. Thus, the final density of particle species i reads

$$n_i(T,\mu_B)=n_i^{\rm primordial}(T,\mu_B)+\sum_a \varrho(i,a)\ n_a^{\rm primordial}(T,\mu_B)\ , \quad (18)$$

where $n_a^{\rm primordial}(T,\mu_B)$ is the thermal density of the a-th particle species at the freeze-out, $\varrho(i,a)$ is the final number of particles of species i which can be received from all possible simple or sequential decays of particle a and the sum is over all species of resonances included in the hadron gas. The values of T and μ_B were fixed for both RHIC energies (*i.e.* $\sqrt{s_{NN}}=130$ and 200 GeV) with the use of data for the most central collisions [5,6]. In the further considerations it is assumed that these values are independent of the centrality. This is reasonable since the very weak centrality dependence of the particle ratios has been observed so far. Recent analyses done in [12,13] have just confirmed the above-mentioned assumption.

The second step of this approach is to determine values of τ and $\rho_{\max}$. Now the k-th measured quantity $R_k^{\exp}$ is the value of ${\rm d}N_i^{\exp}/({\rm d}^2p_T{\rm d}y)|_{\rm mid}$ for measured particle species i and its transverse momentum p_T, whereas the theoretical equivalent $R_k^{\rm th}(\tau,\rho_{\max})$ is given by formula (7). Note that again the χ^2-function depends on two free parameters, now τ and $\rho_{\max}$, since the values of T and μ_B, which were determined early, have been put into eq. (7).

The fitted values of parameters of the model are taken from [5,6] and are gathered in table 1. Since not all bins reported in [14–16] were examined, the lacking values of the geometric parameters have been obtained from the linear approximation between the nearest up and down neighbours. This is justified because the geometric parameters, when plotted as a function of centrality, show roughly linear dependence [6]. Also, in table 1 the corresponding number of participants ($N_{\rm part}$) is given for each bin. If the division into centrality classes is different for the identified-charged-hadron measurements and the ${\rm d}E_T/{\rm d}\eta$ and ${\rm d}N_{\rm ch}/{\rm d}\eta$ measurements, values of $N_{\rm part}$ are taken from reports on the former. Therefore, values of $N_{\rm part}$ from [14,17] are listed for PHENIX, whereas values of $N_{\rm part}$ for STAR are taken from its transverse-energy measurement analysis [9] (in [15,16] numbers of participants are not given).

4 Results

The results of numerical estimations of ${\rm d}N_{\rm ch}/{\rm d}\eta|_{\rm mid}$, eq. (13), divided by the number of participant pairs for PHENIX centrality bins tabulated in table 1 are presented in figs. 1 and 2 for $\sqrt{s_{NN}}=130$ and 200 GeV, respectively. Additionally to the straightforward PHENIX measurements of the total charged-particle multiplicity, also the data from the summing up of the integrated charged-hadron yields are depicted in these figures (more precisely, since the integrated charged-hadron yields are given as rapidity densities, the transformation to pseudo-rapidity should be done, which means the division by a factor 1.2 here, see [18]). This is because fits of the parameters of the model should be done to the same p_T spectra which are to be integrated to deliver the charged-hadron yields. For PHENIX at $\sqrt{s_{NN}}=200$ GeV this is not true since fits were done to the preliminary data [15], but the integrated charged-hadron yields were delivered in the final report [17]. And as one can see from a comparison between figures in [15] and [17], points from the former are slightly above the corresponding points from the latter. To estimate the scale of this difference, the sum of integrated charged-hadron yields at $N_{\rm part}=114.2$ (the point of the biggest discrepancy between the model evaluation and the experimental data, see fig. 2) has been obtained again from digitizing the data depicted in preliminary plots in [15]. This gives 3.31 of charged particles per participant pair, which is exactly 10% above the value

Table 1. Values of thermal and geometric parameters of the model for various centrality bins taken from [5,6]. Marked are these bins, for which values of geometric parameters have been obtained by the author from the linear approximation between the nearest neighbours (see the text for the explanation).

Collision case	Centrality (%)	N_{part}	τ (fm)	$\rho_{\max}$ (fm)
PHENIX at $\sqrt{s_{NN}} = 130$ GeV:	0–5	348	8.20	6.90
$T = 165$ MeV, $\mu_B = 41$ MeV	5–15*	271	7.49	6.30
	15–30	180	6.30	5.30
	30–60*	79	4.62	3.91
	60–92	14	2.30	2.0
PHENIX at $\sqrt{s_{NN}} = 200$ GeV:	0–5	351.4	7.86	7.15
$T = 165.6$ MeV, $\mu_B = 28.5$ MeV	5–10*	299.0	7.48	6.81
	10–15*	253.9	7.10	6.47
	15–20*	215.3	6.71	6.13
	20–30	166.6	6.14	5.62
	30–40	114.2	5.73	4.95
	40–50	74.4	4.75	3.96
	50–60	45.5	3.91	3.12
	60–70	25.7	3.67	2.67
	70–80	13.4	3.09	2.02
STAR at $\sqrt{s_{NN}} = 200$ GeV:	0–5	352	9.74	7.74
$T = 165.6$ MeV, $\mu_B = 28.5$ MeV	5–10	299	8.69	7.18
	10–20	234	8.12	6.44
	20–30	166	7.24	5.57
	30–40	115	7.07	4.63
	40–50	76	6.38	3.91
	50–60	47	6.19	3.25
	60–70*	27	5.70	2.51
	70–80	14	5.21	1.76

obtained from the data given in [17]. And the model evaluation is only 8.5% greater than this number. Also in [17] the feeding of $p\,(\bar{p})$ from $\Lambda\,(\bar{\Lambda})$ decays is excluded, contrary to [15]. Therefore, the model estimates should overestimate the corresponding recalculated experimental values for PHENIX at $\sqrt{s_{NN}} = 200$ GeV. To diminish this effect, integrated p and $\bar{p}$ yields delivered in [17], were corrected to include back the feeding. The correction was done by the division by a factor 0.65, which is a rough average of a p_T-dependent multiplier used by the PHENIX Collaboration (see fig. 4 and eq. (5) in [17]). Since all the just-stated reasons for the "systematic" discrepancies affect the absolute values of $\mathrm{d}N_{\mathrm{ch}}/\mathrm{d}\eta|_{\mathrm{mid}}$, they reveal themselves in the normalization factor τ^3 in the model (see eq. (7)). For PHENIX at $\sqrt{s_{NN}} = 130$ GeV the same spectra were used to fit the model parameters and to obtain the integrated yields [14], so the predictions should agree with the recalculated data in principle. As one can notice from figs. 1 and 2, the above comments concerning both PHENIX measurements are true. The greatest overestimation is in the most peripheral bin and in the midcentrality region of the measurements at $\sqrt{s_{NN}} = 200$ GeV. But even at the worst point the model prediction is 17% over the corresponding recalculated experimental value. It is not so bad because the absolute value of theoretical $\mathrm{d}N_{\mathrm{ch}}/\mathrm{d}\eta$ is determined by the factor τ^3. This means that the 5.3% uncertainty in τ is enough to cause the 17% uncertainty in $\mathrm{d}N_{\mathrm{ch}}/\mathrm{d}\eta$. The second reason for the quantitative disagreement is that transverse-momentum spectra are measured in *limited ranges*, so very important low-p_T regions are not covered by the data. To obtain integrated yields, some extrapolations below and above the measured ranges are used. In fact these extrapolations are only analytical fits, but contributions from regions covered by them account for about 25–40% of the integrated yields [14]. It might turn out that these extrapolations differ from the thermal distributions supplemented by the distributions of products of decays.

Generally, the agreement of the model predictions with the data is much better for RHIC at $\sqrt{s_{NN}} = 130$ GeV. For the case of $\sqrt{s_{NN}} = 200$ GeV, only the rough qualitative agreement has been reached and the reasons have just been explained. It is also worth stressing once more, that the discrepancy between the directly measured $\mathrm{d}N_{\mathrm{ch}}/\mathrm{d}\eta$ and $\mathrm{d}N_{\mathrm{ch}}/\mathrm{d}\eta$ expressed as the sum of the integrated charged-hadron yields can be one of these reasons, especially for RHIC at $\sqrt{s_{NN}} = 200$ GeV (see fig. 2; this

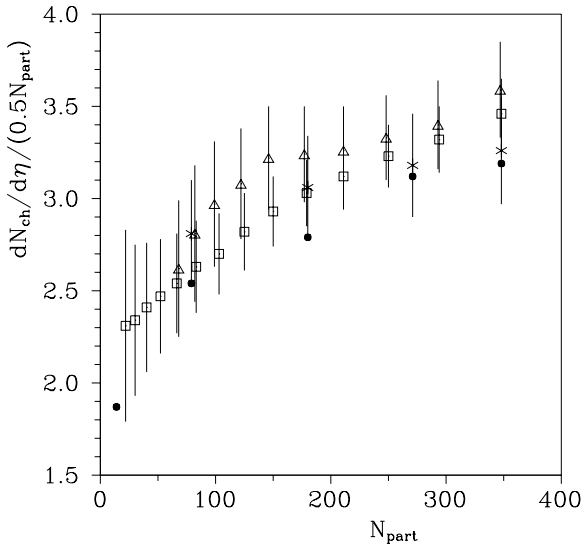

Fig. 1. $\mathrm{d}N_{\mathrm{ch}}/\mathrm{d}\eta$ per pair of participants *versus* N_{part} for RHIC at $\sqrt{s_{NN}} = 130$ GeV. Dots denote model evaluations, squares the newest PHENIX data [10], triangles the earlier reported PHENIX data [7] and crosses are the recalculated PHENIX data from summing up the integrated charged-hadron yields delivered in [14].

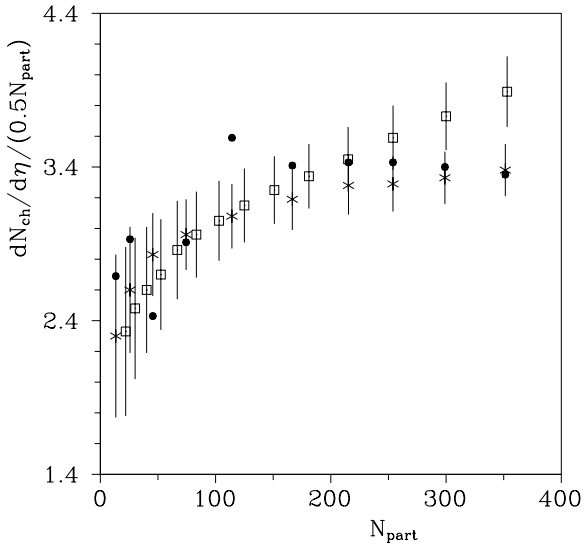

Fig. 2. $\mathrm{d}N_{\mathrm{ch}}/\mathrm{d}\eta$ per pair of participants *versus* N_{part} for RHIC at $\sqrt{s_{NN}} = 200$ GeV. Dots denote model evaluations, squares PHENIX data [10] and crosses are the recalculated PHENIX data from summing up the integrated charged-hadron yields delivered in [17].

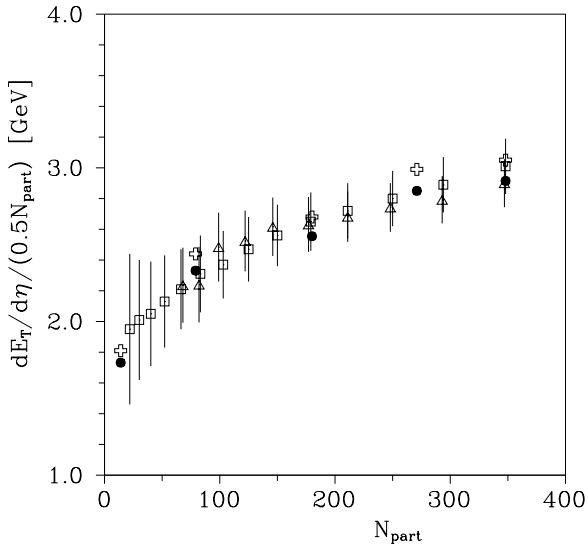

Fig. 3. $\mathrm{d}E_T/\mathrm{d}\eta$ per pair of participants *versus* N_{part} for RHIC at $\sqrt{s_{NN}} = 130$ GeV. Dots and open crosses denote model evaluations, triangles and squares are PHENIX data [7,10]. Dots and triangles are for the older definition of E_T, *i.e.* the total energy E_i is taken also for antibaryons in eq. (1).

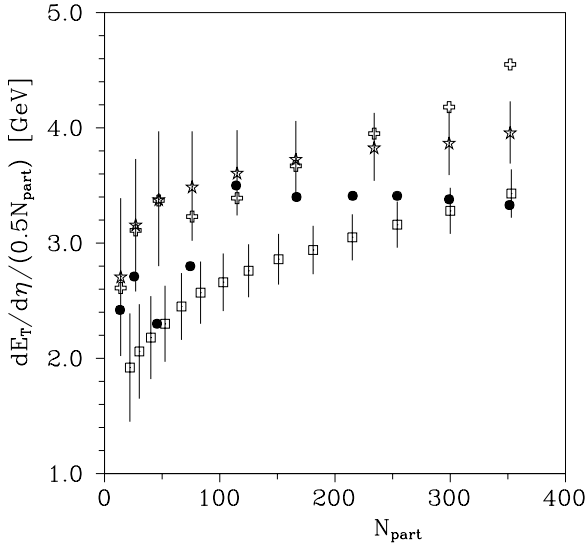

Fig. 4. $\mathrm{d}E_T/\mathrm{d}\eta$ per pair of participants *versus* N_{part} for RHIC at $\sqrt{s_{NN}} = 200$ GeV. Dots and open crosses denote model evaluations, squares and stars are data. Dots and squares are for PHENIX (data from [10]), open crosses and stars for STAR (original data from [9] have been rescaled to $\eta = 0$, see the text for the explanation).

effect has already been notified in backup slides of [15]). The discrepancy starts at midcentrality and rises with the centrality.

The estimates of $\mathrm{d}E_T/\mathrm{d}\eta|_{\mathrm{mid}}$, eq. (14), divided by the number of participant pairs are shown in figs. 3 and 4 for $\sqrt{s_{NN}} = 130$ and 200 GeV, respectively. The quality of the model predictions for $\mathrm{d}E_T/\mathrm{d}\eta$ measured by PHENIX is the same as for $\mathrm{d}N_{\mathrm{ch}}/\mathrm{d}\eta$. Again, only the qualitative agreement has been reached in the case of $\sqrt{s_{NN}} = 200$ GeV but the overestimation is higher and equals 30% at most. The main source of the overestimation seems to be the same as in the $\mathrm{d}N_{\mathrm{ch}}/\mathrm{d}\eta$ case, namely the uncertainty of fitting the parameter τ. The STAR measurements need separate comments. The STAR data were taken not at midrapidity ($\eta = 0$) as in the PHENIX case but at $\eta = 0.5$ on the average [9]. But the p_T spectra used for fits of the geometric parameters were measured at midrapidity, also in the STAR case [16]. Therefore,

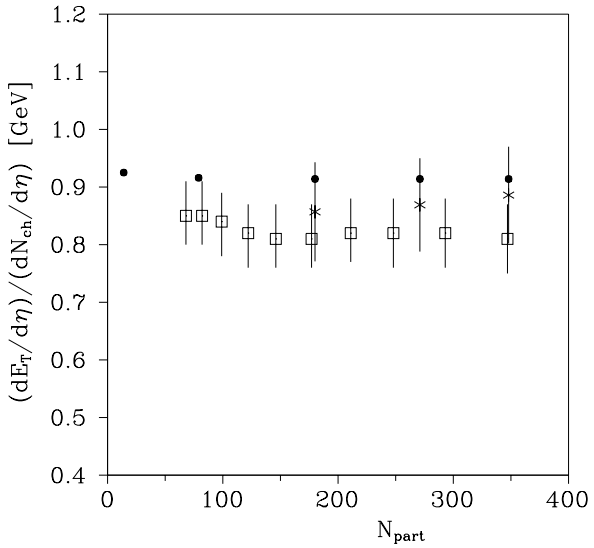

Fig. 5. $\langle dE_T/d\eta\rangle/\langle dN_{ch}/d\eta\rangle$ *versus* N_{part} for RHIC at $\sqrt{s_{NN}} = 130$ GeV and for the older definition of E_T, *i.e.* the total energy E_i is taken also for antibaryons in eq. (1). Dots denote model evaluations, squares are the earlier PHENIX data [8]. Crosses denote recalculated PHENIX data points, *i.e.* the sum of integrated charged-hadron yields [14] has been substituted for the denominator in the ratio.

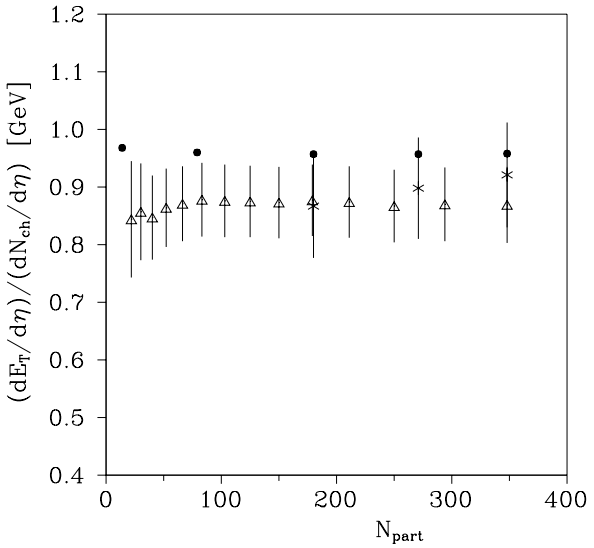

Fig. 6. $\langle dE_T/d\eta\rangle/\langle dN_{ch}/d\eta\rangle$ *versus* N_{part} for RHIC at $\sqrt{s_{NN}} = 130$ GeV. Dots denote model evaluations, triangles are PHENIX data [10]. Crosses denote recalculated PHENIX data points, *i.e.* the sum of integrated charged-hadron yields [14] has been substituted for the denominator in the ratio.

one should expect some "systematic" discrepancy between predictions and the data on the whole. To remove this effect the original STAR data [9] have been divided by a factor $\sin(\theta|_{\eta=0.5}) \approx 0.887$. As can be seen from fig. 4, the predictions and data agree with each other within errors besides the most central point. But even there, the discrepancy does not overcome 15%. Of course, the second source of the quantitative disagreement could be the uncertainty in τ (in fact, as will be seen, it seems to be the main source of the disagreement in all discussed cases).

Figure 4 also shows that both experimental and theoretical values of the transverse energy per participant pair corresponding to the STAR case are $\sim 30\%$ greater than the PHENIX ones. As far as the theoretical estimates are concerned this is the consequence of the higher values of p_T distributions of pions, kaons and antiprotons measured by the STAR Collaboration with respect to PHENIX measurements (it can be seen directly from the careful comparison of the spectra given in [16] and [15]; in fact such a comparison was done in [6], see fig. 5 therein). However, it is difficult to judge without doubts what is the reason for the normalization difference between the experimental data. Additionally, it is interesting that this difference decreases with the centrality. One of the reasons could be a different fiducial aperture: in the PHENIX case, measurements were done for $\mid \eta \mid \leq 0.38$ in pseudo-rapidity and $\Delta\phi = 44.4°$ in azimuth, whereas in the STAR case the pseudo-rapidity range was $0 < \eta < 1$ and the azimuthal coverage $\Delta\phi = 60°$. In both cases the correction factor for fiducial acceptance is given by $1/\Delta\eta \cdot 2\pi/\Delta\phi$, which implicitly assumes the uniform distribution of the raw E_T data in the covered pseudo-rapidity range and in the azimuthal angle. Of course, it might not be exactly true and the final

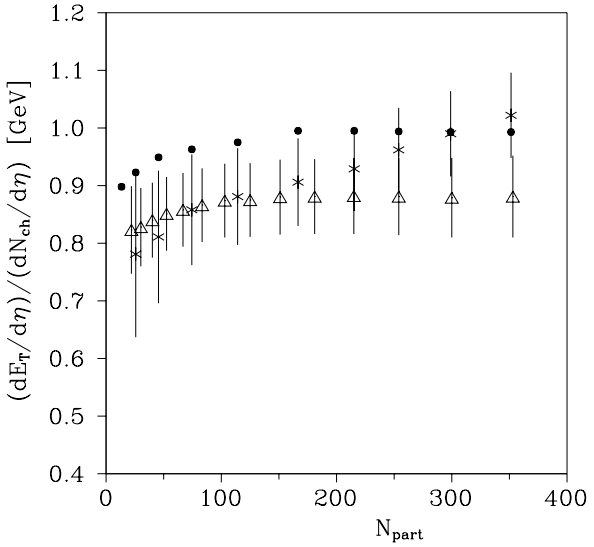

Fig. 7. $\langle dE_T/d\eta\rangle/\langle dN_{ch}/d\eta\rangle$ *versus* N_{part} for RHIC at $\sqrt{s_{NN}} = 200$ GeV. Dots denote model evaluations, triangles are PHENIX data [10]. Crosses denote recalculated PHENIX data points, *i.e.* the sum of integrated charged-hadron yields [17] has been substituted for the denominator in the ratio.

difference in the data could reflect slight deviations from this expected uniformity. Another point is a rather rough technique used by the author to rescale the STAR data to $\eta = 0$. The division by a factor $\sin(\theta|_{\eta=0.5}) \approx 0.887$ contributes almost 13 percentage points to the mentioned $\sim 30\%$ increase in the normalization. Anyway, the increase in the normalization of the transverse-energy measurements observed in the STAR data with respect to the

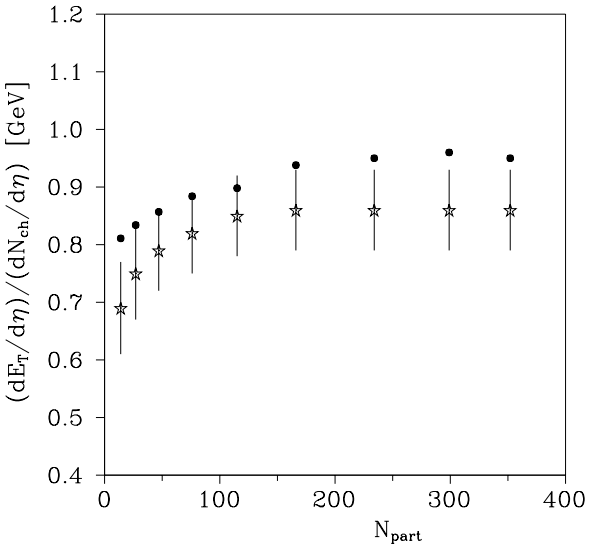

Fig. 8. $\langle dE_T/d\eta\rangle/\langle dN_{ch}/d\eta\rangle$ *versus* N_{part} for RHIC at $\sqrt{s_{NN}} = 200$ GeV. Dots denote model evaluations, stars are STAR data [9].

PHENIX data is consistent with the similar increase in the normalization of the measured spectra.

Values of the ratio $\langle dE_T/d\eta\rangle/\langle dN_{ch}/d\eta\rangle$ as a function of N_{part} are presented in figs. 5-8. As one can see, the position of model predictions is very regular and exactly resembles the configuration of the data in each case, the estimates are only shifted up about 10% as a whole. This indirectly proves that the earlier discussed disagreement in estimates of $dN_{ch}/d\eta|_{mid}$ and $dE_T/d\eta|_{mid}$ has its origin in the uncertainty of fitting the parameter τ (the normalization factor τ^3 cancels in the ratio). The observed 10% overestimation of the ratio can be explained, at least for more central collisions, by the observed discrepancy between the directly measured $dN_{ch}/d\eta$ and $dN_{ch}/d\eta$ expressed as the sum of the integrated charged-hadron yields. If the original data points are replaced by the recalculated data such that the denominators are sums of the integrated charged-hadron yields, then much better agreement can be reached for all but peripheral collisions (see figs. 5-7).

5 Conclusions

The single freeze-out model has been applied to estimate transverse-energy and charged-particle multiplicity densities for different centrality bins of RHIC measurements at $\sqrt{s_{NN}} = 130$ and 200 GeV. These two variables are independent observables, which means that they are measured independently of the identified-hadron spectroscopy. Since model fits were done to identified-hadron data (particle yield ratios and p_T spectra) and transverse-energy and charged-particle multiplicity densities are calculable in the single freeze-out model, it was very tempting to check whether their estimated values agree with the data. Generally the answer is yes, at least on the qualitative level. As has just turned out, the main source of the quantitative disagreement is the uncertainty in the value of the parameter τ. The uncertainty strongly influences both densities since their theoretical equivalents contain the normalization factor τ^3. This conclusion is confirmed by the analysis of the transverse energy per charged particle as a function of the number of participating pairs. The overestimation of at most 30% obtained for the absolute value of the transverse-energy density decreases to the overall overestimation of the order of 10% for the ratio $\langle dE_T/d\eta\rangle/\langle dN_{ch}/d\eta\rangle$. On the quantitative level this means that values of only three parameters of the model are confirmed in the present analysis, namely T, μ_B and the ratio ρ_{max}/τ. Since the ratio is directly connected with the maximum transverse-flow parameter (for the derivation see [1]),

$$\beta_\perp^{max} = \frac{\rho_{max}/\tau}{\sqrt{1+(\rho_{max}/\tau)^2}}\,, \tag{19}$$

this set of parameters is equivalent to T, μ_B and $\beta_\perp^{max}$, which are more commonly used in other statistical models describing particle production in heavy-ion collisions (*e.g.* the blast-wave model [19]).

To summarize, the single freeze-out version of a statistical model fairly well explains the observed centrality dependence of transverse-energy and charged-particle multiplicity pseudo-rapidity densities at midrapidity and their ratio. Also the dependence on $\sqrt{s_{NN}}$ of the above-mentioned variables is well recovered [1]. It should be stressed once more, that this model very well reproduces the particle ratios and the transverse-momentum spectra measured at RHIC [3–6]. In fact, the description of the identified-hadron data was the original motivation for the formulation of the model in [3,4]. The results presented in this paper confirm, in an independent way, the general conclusion drawn in the above-mentioned references, that the single freeze-out model is a very useful (and simple) tool for the estimations of fundamental physical parameters like temperature, chemical potentials or the size of the matter created at the final stages of a heavy-ion collision. This supports the idea of the appearance of a thermal system during such a collision.

This work was supported in part by the Polish Committee for Scientific Research under Contract No. KBN 2 P03B 069 25.

References

1. D. Prorok, Eur. Phys. J. A **24**, 93 (2005).
2. W. Florkowski, W. Broniowski, M. Michalec, Acta Phys. Pol. B **33**, 761 (2002).
3. W. Broniowski, W. Florkowski, Phys. Rev. Lett. **87**, 272302 (2001).
4. W. Broniowski, W. Florkowski, Phys. Rev. C **65**, 064905 (2002).
5. W. Broniowski, A. Baran, W. Florkowski, Acta Phys. Pol. B **33**, 4235 (2002).
6. A. Baran, W. Broniowski, W. Florkowski, Acta Phys. Pol. B **35**, 779 (2004).

7. PHENIX Collaboration (K. Adcox *et al.*), Phys. Rev. Lett. **86**, 3500 (2001).
8. PHENIX Collaboration (K. Adcox *et al.*), Phys. Rev. Lett. **87**, 052301 (2001).
9. STAR Collaboration (J. Adams *et al.*), Phys. Rev. C **70**, 054907 (2004).
10. PHENIX Collaboration (S.S. Adler *et al.*), Phys. Rev. C **71**, 034908 (2005); **71**, 049901 (2005)(E).
11. Particle Data Group Collaboration (K. Hagiwara *et al.*), Phys. Rev. D **66**, 010001 (2002).
12. J. Cleymans, B. Kampfer, M. Kaneta, S. Wheaton, N. Xu, Phys. Rev. C **71**, 054901 (2005).
13. J. Rafelski, J. Letessier, G. Torrieri, Phys. Rev. C **72**, 024905 (2005), nucl-th/0412072.
14. PHENIX Collaboration (K. Adcox *et al.*), Phys. Rev. Lett. **88**, 242301 (2002).
15. PHENIX Collaboration (T. Chujo), Nucl. Phys. A **715**, 151 (2003) and `http://alice-france.in2p3.fr/qm2002/Transparencies/20Plenary/Chujo.ppt`.
16. STAR Collaboration (O. Barannikova, F. Wang), Nucl. Phys. A **715**, 458 (2003).
17. PHENIX Collaboration (S.S. Adler *et al.*), Phys. Rev. C **69**, 034909 (2004).
18. PHENIX Collaboration (A. Bazilevsky), Nucl. Phys. A **715**, 486 (2003).
19. E. Schnedermann, J. Sollfrank, U. Heinz, Phys. Rev. C **48**, 2462 (1993).